THE ASTRONOMICAL JOURNAL, 118:1766–1776, 1999 October

THE REDDENING-FREE DECLINE RATE VERSUS LUMINOSITY RELATIONSHIP FOR TYPE Ia SUPERNOVAE

M. M. PHILLIPS
Las Campanas Observatory, Carnegie Observatories, Casilla 601, La Serena, Chile
PAULINA LIRA
Department of Physics & Astronomy, University of Leicester, Leicester, LE1 7RH, U.K.
NICHOLAS B. SUNTZEFF AND R. A. SCHOMMER
Cerro Tololo Inter-American Observatory, National Optical Astronomy Observatories,[1] Casilla 603, La Serena, Chile
MARIO HAMUY
University of Arizona, Steward Observatory, Tucson, Arizona 85721
AND
JOSÉ MAZA[2]
Departamento de Astronomía, Universidad de Chile, Casilla 36-D, Santiago, Chile
Received 1999 January 27; accepted 1999 July 1

ABSTRACT

We develop a method for estimating the host galaxy dust extinction for type Ia supernovae based on an observational coincidence first noted by Lira, who found that the $B-V$ evolution during the period from 30 to 90 days after V maximum is remarkably similar for all events, regardless of light-curve shape. This fact is used to calibrate the dependence of the $B_{max}-V_{max}$ and $V_{max}-I_{max}$ colors on the light-curve decline rate parameter $\Delta m_{15}(B)$, which can, in turn, be used to separately estimate the host galaxy extinction. Using these methods to eliminate the effects of reddening, we reexamine the functional form of the decline rate versus luminosity relationship and provide an updated estimate of the Hubble constant of $H_0 = 63.3 \pm 2.2$(internal) $\pm$ 3.5(external) km s^{-1} Mpc^{-1}.

Key words: distance scale — supernovae: general

1. INTRODUCTION

In recent years, considerable attention has been focused on the utility of type Ia supernovae (SNe Ia) as cosmological standard candles (e.g., Hamuy et al. 1996b; Perlmutter et al. 1995; Riess, Press, & Kirshner 1996a; Sandage et al. 1996). While there is now abundant evidence for the existence of a significant dispersion in the peak luminosities of these events at optical wavelengths, the absolute magnitudes fortuitously appear to be closely correlated with the decay time of the light curve (Phillips 1993; Hamuy et al. 1995; Riess, Press, & Kirshner 1995; Hamuy et al. 1996a; Riess et al. 1996a). After correction for this effect, dispersions of $\sim$0.15–0.20 mag were obtained by Hamuy et al. (1996b) in the BVI Hubble diagrams of 26 SNe Ia in the redshift range $0.01 \leq z \leq 0.1$, and a Hubble constant of 63.1 $\pm$ 3.4 (internal) $\pm$ 2.9 (external) km s^{-1} Mpc^{-1} was derived via reference to four nearby SNe Ia with Cepheid-calibrated distances. Although Hamuy et al. (1996b) applied a color cut to their sample to eliminate the reddest events, no corrections were applied for possible host galaxy dust extinction of the supernovae in either the distant or nearby samples. Not only might this affect the derived slope of the decline rate versus luminosity relation, but the correctness of the Hubble constant depends on the assumption that the mean reddening of the 26 distant SNe Ia in the Hubble flow is essentially the same as that of the four nearby calibrating SNe.

In a parallel study that included many of the objects observed by Hamuy et al. (1996b), Riess et al. (1996a) developed an empirical method that they called multicolor light-curve shapes (MLCS) to estimate simultaneously the luminosity, distance, and total extinction of each SN Ia. MLCS employs linear estimation algorithms to create a family of SN Ia light curves and color curves and offers considerable elegance in error modeling. However, this first implementation by Riess et al. (1996a) was based on essentially the same "training set" of only nine nearby supernovae used by Phillips (1993), which suffered from uncertain extinction estimates and inhomogeneous secondary distance indicators. This training set was sufficient to determine the existence of the relations between SN Ia light-curve shape, color, and luminosity but not ideal for determining the precise values of these relations. Indeed, a recent reanalysis of MLCS in the B and V bands by Riess et al. (1998), using a much larger training set as well as redshifts as the distance indicator to determine the SN Ia luminosities, improves the precision of the method. Additionally, this reanalysis reduces the strong relation between light-curve shape and $B-V$ color at maximum light initially found by Phillips (1993) and Riess et al. (1996a).

In this paper, we seek to establish an independent procedure for determining host galaxy reddenings for SNe Ia using an observational coincidence first noted by Lira (1995). This method is developed in § 2 and used to estimate the intrinsic $B_{max}-V_{max}$ and $V_{max}-I_{max}$ colors for a sample of $\sim$60 well-observed SNe Ia. We then apply this informa-

[1] Cerro Tololo Inter-American Observatory, National Optical Astronomy Observatories, operated by the Association of Universities for Research in Astronomy, Inc., under cooperative agreement with the National Science Foundation.
[2] Cátedra Presidencial de Ciencias (Chile) 1995.

tion in § 3 to derive reddening-free relations between the decline rate parameter $\Delta m_{15}(B)$ (Phillips 1993) and the peak absolute magnitudes in BVI and to update our estimate of the value of the Hubble constant.

2. COLOR EXCESSES AND INTRINSIC COLORS

2.1. $E(B-V)_{\rm Tail}$

In comparing the color evolution of several apparently unreddened SNe Ia representing the full range of observed light-curve decline rates, Lira (1995) found that the $B-V$ colors at 30–90 days past V maximum evolved in a nearly identical fashion. This property, which was independently discerned by Riess et al. (1996a), is illustrated in Figure 1, where we plot the $B-V$ color evolution from Cerro Tololo Inter-American Observatory photometry of six SNe Ia covering a wide range of decline rates ($0.87 \leq \Delta m_{15}(B) \leq 1.93$) and which likely suffered little or no reddening from dust in their host galaxies. The likelihood of a supernova being unreddened was judged by three basic criteria: (1) the absence of interstellar Na I or Ca II lines in moderate-resolution, high signal-to-noise spectra, (2) the morphology of the host galaxy (SNe that occur in E or S0 galaxies are less likely to be significantly affected by dust), and (3) the position of the supernova in the host galaxy (SNe lying outside the arms and disks of spirals are more likely to have low dust reddening). As discussed by Lira, it is not surprising that the colors of SNe Ia at these late epochs are so similar because their spectra also display an impressive uniformity. This is precisely the epoch where the Fe-Ni-Co core dominates the spectrum that is rapidly evolving into the "supernebula" phase (see Phillips et al. 1992).

From a least-squares fit to the photometry of four of the SNe displayed in Figure 1 (1992A, 1992bc, 1992bo, and 1994D), Lira derived the following relation to describe the intrinsic $B-V$ color evolution

$$(B-V)_0 = 0.725 - 0.0118(t_V - 60)\ , \qquad (1)$$

where t_V is the phase measured in days since V maximum. This fit, which is plotted in Figure 1, is valid over the phase interval $30 \leq t_V \leq 90$ and can be applied to any SN Ia with BV coverage extending to at least $t_V = 30$ days to derive an estimate of the color excess $E(B-V)$. Note in Figure 1 that individual SNe can display systematic residuals with respect to the Lira fit (i.e., the points lie mostly bluer or redder than the line), suggesting that there is an intrinsic dispersion about equation (1). This dispersion amounts to 0.04 mag for the four SNe used by Lira and 0.06 mag for the six SNe shown in Figure 1; in calculating color excesses from equation (1), we will adopt a value of 0.05 mag in our error analysis.

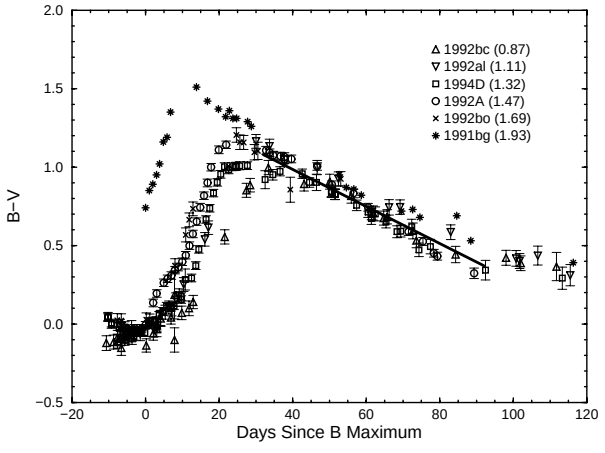

FIG. 1.—$B-V$ color evolution for six SNe Ia that likely suffered little or no reddening from dust in their host galaxies. These six events, whose $\Delta m_{15}(B)$ parameters are indicated in parentheses, cover a wide range of initial decline rates and peak luminosities. The solid line corresponds to the Lira (1995) fit (eq. [1]) to the color evolution during the phase interval $30 \leq t_V \leq 90$. The epoch of $B_{\rm max}$ is assumed to occur 2 days before the epoch of $V_{\rm max}$ (Leibundgut 1988).

For relatively bright SNe observed with CCDs, the precision of the photometry obtained at $\sim$1–3 months after maximum is typically still quite good (0.02–0.05 mag). However, for more distant events, the late-time photometry coverage tends to be relatively sparse, with typical errors $\sim$0.1–0.2 mag for individual observations, and values of $E(B-V)$ derived directly from equation (1) will often have large associated errors. For such SNe, a better technique is to use template fits of the type employed by Hamuy et al. (1996c) to derive an estimate of the observed $B-V$ color at some fiducial epoch in the interval $30 \leq t_V \leq 90$. This value can then be compared with the intrinsic color predicted by equation (1) for the same epoch to derive the color excess. This procedure has the advantage of using the entire set of BV photometry to estimate a late-epoch color rather than just the subset of data obtained at $30 \leq t_V \leq 90$.

For a sample of 62 well-observed SNe Ia with $z \leq 0.1$ consisting of (1) the "Calán/Tololo" sample of 29 SNe Ia published by Hamuy et al. (1996c), (2) 20 SNe Ia published in Riess et al. (1999), which we will refer to as the "CfA" sample, and (3) 13 nearby, well-observed SNe Ia (1937C, 1972E, 1980N, 1981B, 1986G, 1989B, 1990N, 1991T, 1991bg, 1992A, 1994D, 1996X, and 1996bu; see Table 1 for photometry references), we have calculated color excesses

TABLE 1

PHOTOMETRY REFERENCES FOR NEARBY SNE Ia

SN	References
1937C	1
1972E	2–5
1980N	6
1981B	7–9
1986G	10
1989B	11
1990N	12
1991T	12
1991bg	13, 14
1992A	15
1994D	16
1996X	17
1998bu	18

REFERENCES.—(1) Pierce & Jacoby 1995; (2) Ardeberg & de Grood 1973; (3) Cousins 1972; (4) Eggen & Phillips (unpublished); (5) Lee et al. 1972; (6) Hamuy et al. 1991; (7) Barbon, Ciatti, & Rosino 1982; (8) Buta & Turner 1983; (9) Tsvetkov 1982; (10) Phillips et al. 1987; (11) Wells et al. 1994; (12) Lira et al. 1998; (13) Filippenko et al. 1992; (14) Leibundgut et al. 1993; (15) Suntzeff et al. (unpublished); (16) Smith et al. (unpublished); (17) Covarrubias et al. (unpublished); (18) Suntzeff et al. 1999.

from equation (1) via the two techniques described above—i.e., both directly from the late-time photometry and via light-curve template fits. In the following, we will refer to these as the "Direct" and "Template" methods, respectively. For the "Template" method, we chose $t_V = 53$ days as the fiducial reference epoch for which equation (1) predicts $(B-V)_0 = 0.808$. To calculate the host galaxy reddening, $E(B-V)_{\rm host}$, the observed supernova color evolution must be corrected for both Galactic reddening and the effect of redshift (the "K-correction") via the equation

$$(B-V)_{\rm corr} = (B-V)_{\rm obs} - E(B-V)_{\rm Gal} - K_{B-V}\,, \qquad (2)$$

where $(B-V)_{\rm obs}$ is the observed color, $E(B-V)_{\rm Gal}$ is the Galactic reddening, for which we use the values from Schlegel, Finkbeiner, & Davis (1998), and K_{B-V} is the K-correction. The host galaxy reddening is then given by

$$E(B-V)_{\rm host} = (B-V)_{\rm corr} - (B-V)_0\,. \qquad (3)$$

As discussed by Riess et al. (1998) and Nugent et al. (1999), K_{B-V} is not only a function of redshift but also the SN color. Because we are concentrating on an epoch where all SNe Ia show essentially the same $B-V$ color, we need only worry about color differences arising from different amounts of host galaxy reddening. In principle, an iterative procedure should be followed where K_{B-V} for zero host galaxy reddening (Hamuy et al. 1993) is taken as a first guess, $E(B-V)_{\rm host}$ is calculated via equations (2) and (3), and the K_{B-V} correction is then adjusted if $E(B-V)_{\rm host}$ is found to be significantly greater than zero. However, for the range of host galaxy reddenings [$E(B-V) < 0.8$] typical of our sample, the variation of K_{B-V} due to this effect is only 0.00–0.02 mag. This is much smaller than the precision of our reddening indicator, and so we therefore adopt the K_{B-V} corrections for zero extinction with no iteration.

As pointed out by Kim (1997), the observed color excess of an SN Ia will vary slightly with light-curve phase because of the significant color evolution that these events undergo. There will also be a generally smaller dependence on the total amount of dust extinction itself (e.g., Blanco 1956). Using the IRAF task DEREDDEN, which employs a standard Galactic interstellar reddening curve (Cardelli, Clayton, & Mathis 1989), and a program that we have developed for deriving synthetic photometry from spectra, we have calculated observed color excesses as a function of both the light-curve phase and the "true" reddening, $E(B-V)_{\rm true}$, for a database of more than 30 SNe Ia spectra, to characterize and correct for these effects. Note that $E(B-V)_{\rm true}$ parameterizes the amount of extinction along a particular line of sight and *not* the observed color excess that, as stated, will vary as a function of phase and reddening. To convert from $E(B-V)_{\rm obs}$ to $E(B-V)_{\rm true}$ at $t_V = 53$ days, our reference epoch for the "tail" evolution phase, we find the following approximate relation to be valid:

$$E(B-V)_{\rm true} = 1.018/[1/E(B-V)_{\rm obs} - 0.072]\,. \qquad (4)$$

The observed decline rate of an SN Ia will also be a weak function of the dust extinction, which affects the light curves. This follows from Figure 2, where we have used the above-described calculations to examine the variation of

$$R_B = A_B/E(B-V)_{\rm true} \qquad (5)$$

with light-curve phase for three different values of $E(B-V)_{\rm true}$. In this equation, A_B is the *observed* extinction,

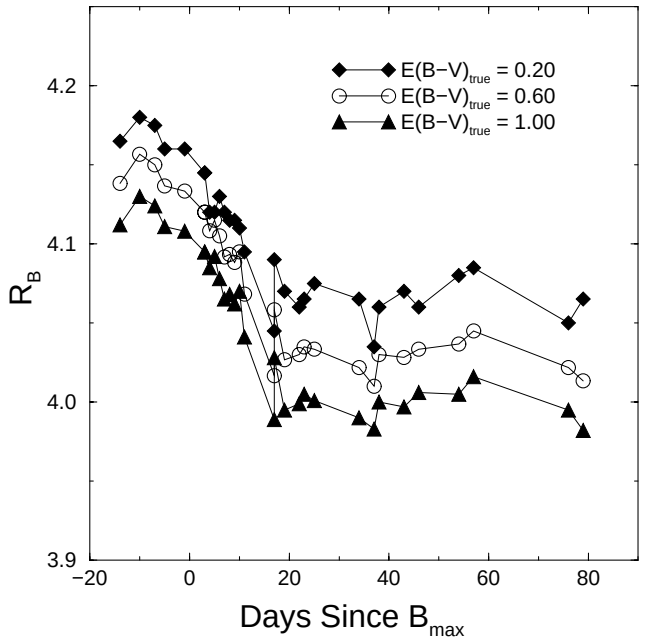

FIG. 2.—Variation of $R_B = A_B/E(B-V)_{\rm true}$ as a function of phase for different values of $E(B-V)_{\rm true}$. Note that A_B is the observed extinction in B, which is a function of the light-curve phase.

which is equal to the difference between the synthetic B magnitudes calculated for a reddened and unreddened spectrum. Combining equation (5) with the definition of the observed decline rate parameter,

$$\Delta m_{15}(B)_{\rm obs} = B_{\rm obs}(+15\ {\rm days}) - B_{\rm obs}({\rm max})\,,$$

gives

$$\Delta m_{15}(B)_{\rm obs} = \Delta m_{15}(B)_{\rm true} + [R_B(+15\ {\rm days}) - R_B({\rm max})]E(B-V)_{\rm true}\,.$$

From Figure 2, this can be shown to reduce to the following approximate relation:

$$\Delta m_{15}(B)_{\rm true} \simeq \Delta m_{15}(B)_{\rm obs} + 0.1E(B-V)_{\rm true}\,. \qquad (6)$$

Note that reddening acts to *decrease* the decline rate, which is opposite to the conclusion of Leibundgut (1988), who employed a formula from Schmidt-Kaler (1982), which gives A_B as a function of the intrinsic color, $(B-V)_0$ and the observed color excess, $E(B-V)_{\rm obs}$. Although this formula was derived for normal stars, it does a surprisingly reasonable job of predicting the shape of the variations of A_B with light-curve phase implied by Figure 2. However, to use this formula correctly, one must take into account that $E(B-V)_{\rm obs}$ also varies with phase; Leibundgut (1988) assumed that $E(B-V)_{\rm obs}$ was constant with phase, which led him to incorrectly conclude that the effect of reddening was to increase the decline rate.

Figure 3 illustrates application of the "Direct" and "Template" methods to the photometry of two representative SNe observed in the course of the Calán/Tololo survey. Comparison of the $E(B-V)_{\rm host}$ values (converted to "true" reddenings via eq. [4]) derived via both techniques for 54 of the SNe in our sample is shown in Figure 4. In general, there is good agreement between the two reddening determinations, with no evidence for a difference in zero points (the weighted average of the difference amounts to 0.01 ± 0.01). The most discrepant points correspond to SNe 1992ag and 1996ai (not plotted). SN 1992ag, which was

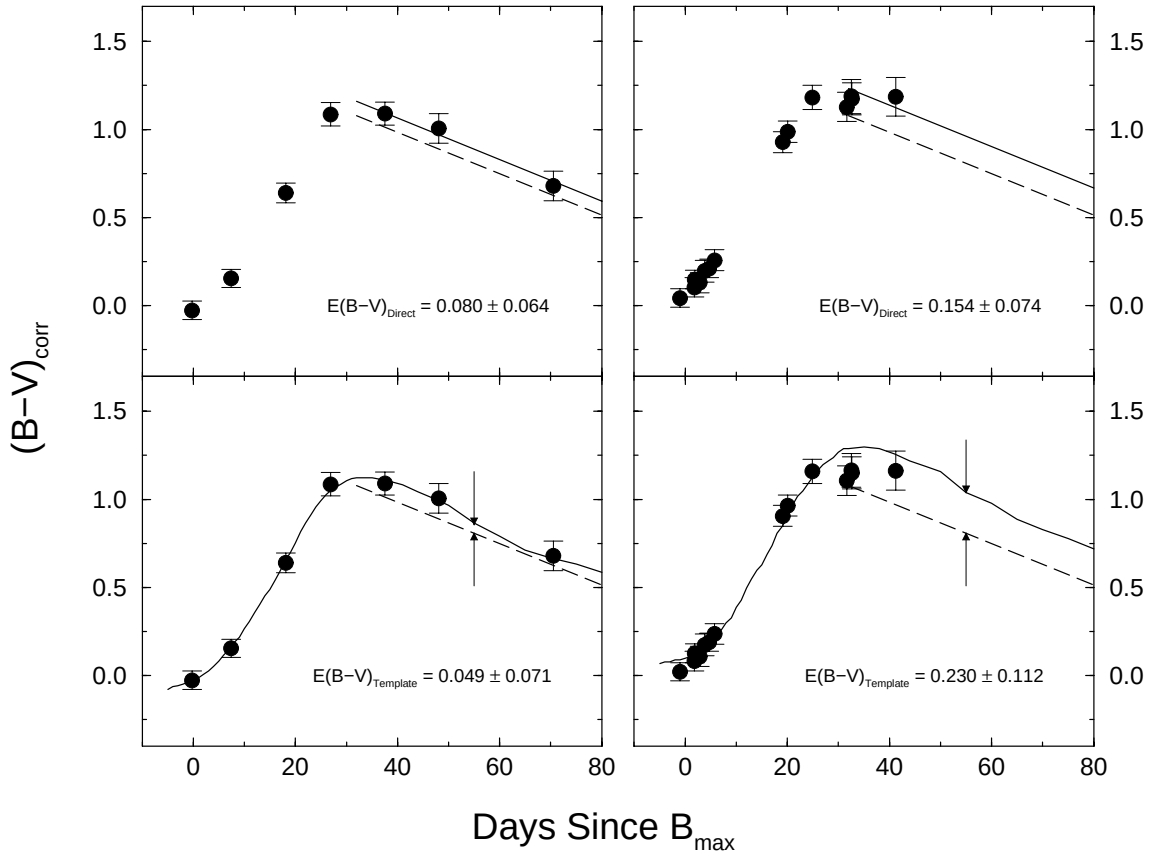

FIG. 3.—Illustration of the "Direct" (*upper panels*) and "Template" (*lower panels*) techniques for estimating the host galaxy reddening of SNe Ia from the $B-V$ evolution during the phase interval $30 \leq t_V \leq 90$. The photometry for SN 1900O (*left*) and SN 1992bh (*right*) is from Hamuy et al. (1996c) and has been corrected for both Galactic reddening and the K-correction. The dashed line in each graph corresponds to the Lira (1995) fit (eq. [1]) to the color evolution of unreddened SNe Ia. The solid lines in the upper panels are the Lira relation shifted to fit the photometry of the SNe in the interval $30 \leq t_V \leq 90$; $E(B-V)_{\rm Direct}$ is then defined as the difference between the solid and dashed lines. In the lower panels, the solid lines represent the template fits derived by Hamuy et al. (1996c) to the corrected photometry. The value of $E(B-V)_{\rm Template}$ is defined as the difference between the template fits and the unreddened Lira relation (*dashed lines*) at $t_V = 53$ days ($t_B \simeq 55$ days).

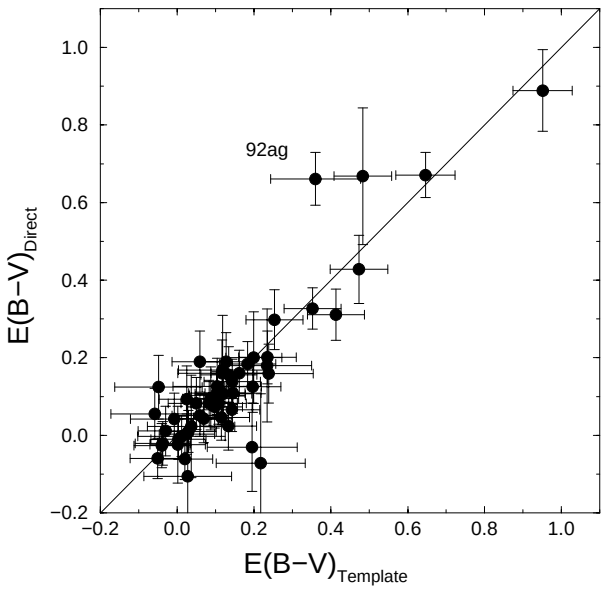

FIG. 4.—Comparison of color excesses calculated via the "Direct" and "Template" methods from the $B-V$ evolution during the phase interval $30 \leq t_V \leq 90$.

discovered and observed in the Calán/Tololo survey, occurred near the center of an edge-on spiral host galaxy, and we suspect that the B photometry obtained at late epochs was systematically affected by the difficulty of subtracting the host galaxy. A similar explanation may apply to the severely reddened SN 1996ai, for which we find $E(B-V)_{\rm Template} = 1.97 \pm 0.08$ and $E(B-V)_{\rm Direct} = 2.43 \pm 0.19$; in this case, the $E(B-V)_{\rm Direct}$ estimate is based on a single color measurement, which we suspect may be more uncertain than the formal photometry errors would suggest.

The zero point of these color excesses can be checked by examining the reddenings obtained for the subset of SNe Ia with E/S0 host galaxies, where we expect there to be little or no host galaxy dust.[3] For the 21 SNe Ia in our sample with E/S0 hosts, we defined $E(B-V)_{\rm Tail}$ to be the weighted

[3] Although there is some evidence for a diffuse component of dust in nearby E galaxies that would be difficult to detect directly (e.g., Goudfrooij & de Jong 1995), the SNe with E hosts in our sample occurred at relatively large projected distances (≥ 10 kpc) from the centers of their host galaxies where the maximum amount of reddening consistent with observed color gradients is typically $E(B-V) \leq 0.05$ (Wise & Silva 1996). Thus, it seems reasonable to expect that SNe in E galaxies should give a reliable determination of the reddening zero point.

mean of the host galaxy color excesses $E(B-V)_{\rm Template}$ and $E(B-V)_{\rm Direct}$.[4] We find an average value of $E(B-V)_{\rm Tail} = 0.05 \pm 0.03$, which decreases to 0.03 ± 0.03 if we limit the sample to the eight SNe in E galaxies. We do not consider either of these results to be significantly different from zero. Moreover, there are additional arguments for retaining the Lira zero point:

1. The SNe used to determine the Lira zero point were all relatively nearby. We therefore have precise morphological classifications for the host galaxies. Being nearby, it is also easier to see signs of dust directly in the host galaxies. In addition, we have high signal-to-noise spectra that allow us to put limits on the amount of interstellar gas present in the line of sight. Although Lira used only four SNe for her zero point, the six shown in Figure 1 give the same zero point to 0.01 mag.

2. Of the 21 SNe in our sample with E/S0 host galaxies, many are relatively distant. Some of the morphological classifications of the hosts could therefore be in error (e.g., at large distances it is sometimes difficult to distinguish an S0 galaxy from an Sa). Hence, we cannot be certain that some of these galaxies do not have significant dust. Also, very few of the spectra obtained of these SNe have sufficient signal-to-noise to look for interstellar absorption lines.

Thus, we adopt the zero point of equation (1) without modification. In any case, it should be recalled that the precision of any single measurement of $E(B-V)_{\rm Tail}$ will be limited by the intrinsic dispersion about equation (1), which, as stated earlier, appears to be $\sim$0.04–0.06 mag.

2.2. $E(B-V)_{\rm max}$ and $E(V-I)_{\rm max}$

The "tail" evolution of the intrinsic $B-V$ color as an indicator of host galaxy dust reddening offers the advantage of being insensitive to the initial decline rate (or luminosity) of the SN, but the obvious disadvantage of this method is that it requires the light curves to be followed to several magnitudes below maximum light, which in practice is often impossible for distant SNe Ia. Ideally, we would prefer to be able to use the maximum-light colors to determine the host galaxy reddening. As is seen in Figure 1 (and pointed out by Lira 1995), the $B-V$ colors at maximum light of most SNe Ia show a fairly small dispersion, although the fastest declining events (such as 1991bg) are clearly significantly redder. In principle, we can calibrate any dependence on decline rate by using the "Tail" method to identify a sample of unreddened SNe Ia representing a wide range of initial decline rates.

Columns (2)–(4) of Table 2 list the measured decline rate parameter $\Delta m_{15}(B)_{\rm obs}$, the color excess $E(B-V)_{\rm Gal}$ due to Galactic reddening, and the $E(B-V)_{\rm Tail}$ values calculated as per § 2.1 for the 62 SNe Ia in our full sample. We find that a total of 20 events have values of $E(B-V)_{\rm Tail} < 0.06$—i.e., less than or equal to the standard deviation of a single reddening measurement. In the following, we will assume that these SNe Ia were essentially unreddened by dust in their host galaxies. The "colors" $B_{\rm max}-V_{\rm max}$ and $V_{\rm max}-I_{\rm max}$ for these 20 events are plotted versus the decline rate parameter $\Delta m_{15}(B)$ in Figure 5. Here we differentiate between those SNe Ia with light-curve coverage beginning less than 7 days after the epoch of $B_{\rm max}$ and those for which the first observation was not obtained until more than 7 days after the epoch of $B_{\rm max}$, as we expect that the color excesses determined for the latter SNe will be less precise than those for events observed within a week of maximum light. For decline rates in the range $0.9 \leq \Delta m_{15}(B) \leq 1.6$, the variation in color is approximately linear in both colors. The fastest-declining events, 1991bg and 1992K, clearly do not follow this trend, presumably because of the appearance in their spectra of strong absorption features of low-ionization species such as Ti II as a consequence of lower effective temperatures (see Nugent et al. 1995).

Over the linear portion of the relations shown in Figure 5, we calculate the following weighted, least-squares fits to the SNe Ia with light-curve coverage beginning less than 7 days after $B_{\rm max}$:

$$(B_{\rm max}-V_{\rm max})_0 = -0.070(\pm 0.012) + 0.114(\pm 0.037) \times [\Delta m_{15}(B) - 1.1],\ \sigma = 0.030,\ n = 14\ ; \quad (7)$$

$$(V_{\rm max}-I_{\rm max})_0 = -0.323(\pm 0.017) + 0.250(\pm 0.056) \times [\Delta m_{15}(B) - 1.1],\ \sigma = 0.042,\ n = 11\ . \quad (8)$$

These fits are plotted as solid lines in Figure 5. For reference, we also show the relations derived by Phillips (1993) and Hamuy et al. (1996a), the original formulation of MLCS (Riess et al. 1996a), and the revised version of Riess et al. (1998). Clearly the slopes of the $B_{\rm max}-V_{\rm max}$ relations found by Phillips (1993) and the original MLCS are too steep, whereas both the Hamuy et al. (1996a) and the new MLCS provide much better approximations to the data. The small offset between our fit and that of Riess et al. (1998) is due in part to our usage of the Schlegel et al. (1998) Galactic reddenings, which are on average $\sim$0.02 mag greater than the Burstein & Heiles (1982) values employed by Riess et al. (1998); the larger offset with respect to the Hamuy et al. (1996a) fits is due to the same effect and also to the fact that Hamuy et al. (1996a) did not correct their data for host galaxy extinction. Curiously, the Phillips (1993) relation for $V_{\rm max}-I_{\rm max}$ is a poor fit to the data, whereas the original MLCS reproduces the dependence quite well.

To use the relations given by equations (7) and (8) to estimate host galaxy reddenings, we proceed in a fashion analogous to that described in § 2.1. The observed color excess is defined as

$$E(B-V)_{\rm host} = (B_{\rm max}-V_{\rm max})_{\rm corr} - (B_{\rm max}-V_{\rm max})_0\ , \quad (9)$$

where $(B_{\rm max}-V_{\rm max})_{\rm corr}$ is given by

$$(B_{\rm max}-V_{\rm max})_{\rm corr} = (B_{\rm max}-V_{\rm max})_{\rm obs} - E(B-V)_{\rm Gal} - K_{B_{\rm max}-V_{\rm max}}\ . \quad (10)$$

In principle, because $\Delta m_{15}(B)_{\rm obs}$ is a function of the reddening, equations (9) and (10) should be employed in an

[4] In taking a weighted mean of $E(B-V)_{\rm Direct}$ and $E(B-V)_{\rm Template}$, we have assumed these to be independent measurements of the reddening. Technically speaking, this is not fully the case, since the tail photometry used to measure $E(B-V)_{\rm Direct}$ is a subset of the entire photometry set we use in calculating $E(B-V)_{\rm Template}$. However, for a typical SN in our sample, the tail data amount to less than half the full set of photometry and enter into the template fits with low weight because of their larger measurement errors.

TABLE 2

HOST GALAXY REDDENINGS

SN (1)	$\Delta m_{15}(B)_{obs}$[a] (2)	$E(B-V)^{b}_{Gal}$ (3)	$E(B-V)^{b}_{Tail}$ (4)	$E(B-V)^{b}_{max}$ (5)	$E(V-I)^{b}_{max}$ (6)	$E(B-V)^{a}_{Avg}$ (7)
1937C.....	0.87(10)	0.014(001)	0.012(053)	0.061(060)	...	0.03(03)
1972E.....	0.87(10)	0.056(006)	−0.003(051)	0.040(060)	−0.001(073)	0.01(03)
1980N	1.28(04)	0.021(002)	0.110(052)	0.077(044)	−0.009(056)	0.05(02)
1981B.....	1.10(07)	0.018(002)	0.084(053)	0.150(044)	...	0.11(03)
1986G	1.73(07)	0.115(011)	0.668(057)	...	...	0.50(05)
1989B.....	1.31(07)	0.032(003)	0.457(067)	0.363(069)	0.465(077)	0.34(04)
1990N	1.07(05)	0.026(003)	0.160(057)	0.106(051)	0.057(061)	0.09(03)
1990O	0.96(10)	0.093(009)	0.069(060)	0.072(061)	−0.071(073)	0.02(03)
1990T.....	1.15(10)	0.053(005)	0.138(056)	0.080(104)	0.052(112)	0.09(04)
1990Y.....	1.13(10)	0.008(001)	0.348(061)	0.388(106)	0.064(111)	0.23(04)
1990af	1.56(05)	0.035(004)	−0.008(111)	0.052(047)	...	0.04(03)
1991S	1.04(10)	0.026(003)	0.122(069)	0.089(104)	0.004(111)	0.06(04)
1991T.....	0.94(05)	0.022(002)	0.174(052)	...	...	0.14(05)[c]
1991U	1.06(10)	0.062(006)	0.145(063)	0.141(105)	0.152(112)	0.11(04)
1991ag	0.87(10)	0.062(006)	0.075(054)	0.122(061)	0.030(080)	0.07(03)
1991bg.....	1.93(10)	0.040(004)	0.038(064)	...	...	0.03(05)
1992A.....	1.47(05)	0.017(002)	0.004(051)	0.000(046)	−0.061(059)	0.00(02)
1992J	1.56(10)	0.057(006)	0.050(065)	0.129(106)	−0.064(114)	0.03(04)
1992K	1.93(10)	0.101(010)	−0.029(055)	...	...	0.00(04)
1992P.....	0.87(10)	0.021(002)	0.082(058)	0.064(046)	0.093(072)	0.07(03)
1992ae	1.28(10)	0.036(004)	0.215(097)	0.132(060)	...	0.12(04)
1992ag	1.19(10)	0.097(010)	0.622(066)	0.151(061)	0.116(072)	0.10(04)[d]
1992al	1.11(05)	0.034(003)	0.052(053)	−0.015(044)	−0.013(068)	0.01(03)
1992aq.....	1.46(10)	0.012(001)	0.137(096)	0.115(061)	−0.200(074)	0.00(04)
1992au.....	1.49(10)	0.017(002)	0.031(093)	0.058(105)	−0.243(113)	0.00(04)
1992bc.....	0.87(05)	0.022(002)	−0.055(053)	−0.006(044)	0.012(069)	0.00(02)
1992bg.....	1.15(10)	0.185(018)	0.050(059)	0.009(062)	−0.016(075)	0.01(03)
1992bh.....	1.05(10)	0.022(002)	0.177(071)	0.132(060)	0.126(071)	0.12(03)
1992bk.....	1.57(10)	0.015(001)	0.034(065)	0.001(062)	−0.013(114)	0.01(03)
1992bl	1.51(10)	0.011(001)	−0.006(065)	0.012(061)	−0.073(075)	0.00(03)
1992bo.....	1.69(05)	0.027(003)	−0.004(058)	−0.014(049)	0.020(064)	0.00(03)
1992bp.....	1.32(10)	0.069(007)	0.145(077)	−0.034(060)	−0.090(073)	0.00(03)
1992br	1.69(10)	0.026(003)	−0.002(102)	0.016(063)	...	0.01(04)
1992bs	1.13(10)	0.012(001)	0.142(102)	0.123(060)	...	0.10(04)
1993B.....	1.04(10)	0.079(008)	0.200(069)	0.196(061)	0.047(072)	0.12(03)
1993H	1.69(10)	0.060(006)	0.064(057)	...	...	0.05(04)
1993O	1.22(05)	0.053(005)	0.059(059)	−0.046(044)	0.025(069)	0.00(03)
1993ac	1.19(10)	0.163(016)	0.080(089)	0.096(062)	0.250(074)	0.12(04)
1993ae	1.43(10)	0.039(004)	−0.024(053)	−0.036(104)	−0.009(113)	0.00(03)
1993ag	1.32(10)	0.112(011)	0.152(061)	0.112(061)	−0.025(074)	0.07(03)
1993ah.....	1.30(10)	0.020(002)	0.075(074)	−0.013(104)	−0.062(112)	0.01(04)
1994D	1.32(05)	0.022(002)	−0.060(052)	−0.017(044)	−0.010(057)	0.00(02)
1994M	1.44(10)	0.024(002)	0.115(064)	0.057(061)	0.126(074)	0.08(03)
1994Q	1.03(10)	0.017(002)	0.090(065)	0.099(104)	0.048(111)	0.06(04)
1994S	1.10(10)	0.021(002)	0.001(112)	0.009(045)	−0.034(071)	0.00(03)
1994T.....	1.39(10)	0.029(003)	0.105(114)	0.126(061)	0.112(073)	0.09(04)
1994ae	0.86(05)	0.031(003)	0.184(056)	0.175(045)	0.053(057)	0.12(03)
1995D	0.99(05)	0.058(006)	0.103(054)	0.044(044)	0.016(056)	0.04(02)
1995E.....	1.06(05)	0.027(003)	0.934(072)	0.793(045)	0.992(068)	0.74(03)
1995ac	0.91(05)	0.042(004)	0.109(054)	...	...	0.08(04)[c]
1995ak.....	1.26(10)	0.043(004)	0.260(057)	0.107(060)	0.294(072)	0.18(03)
1995al	0.83(05)	0.014(001)	0.157(064)	0.246(045)	...	0.15(03)
1995bd.....	0.84(05)	0.495(050)	0.242(074)	...	...	0.15(06)[c]
1996C.....	0.97(10)	0.014(001)	0.078(055)	0.139(060)	0.106(072)	0.09(03)
1996X.....	1.25(05)	0.069(007)	−0.010(051)	−0.016(044)	0.076(056)	0.01(02)
1996Z.....	1.22(10)	0.063(006)	0.500(073)	0.352(061)	...	0.33(04)
1996ai	0.99(10)	0.014(001)	2.015(080)	1.936(065)	1.575(072)	1.44(04)
1996bk.....	1.75(10)	0.018(002)	0.274(064)	...	...	0.19(05)
1996bl	1.17(10)	0.105(011)	0.113(063)	0.095(061)	0.090(073)	0.08(03)
1996bo.....	1.25(05)	0.078(008)	0.358(053)	0.385(061)	0.253(069)	0.28(03)
1998bu.....	1.01(05)	0.025(003)	0.328(053)	0.375(054)	0.519(074)	0.33(03)
1996bv.....	0.93(10)	0.105(010)	0.215(062)	0.233(061)	0.318(073)	0.21(03)

[a] Mean errors are listed in units of 0.01 mag.

[b] Mean errors are listed in units of 0.001 mag.

[c] 1991T-like event; $E(B-V)_{Avg}$ based only on value of $E(B-V)_{Tail}$.

[d] $E(B-V)_{Tail}$ measurement ignored in calculation of $E(B-V)_{Avg}$ because of the likelihood of systematic errors in late-time photometry.

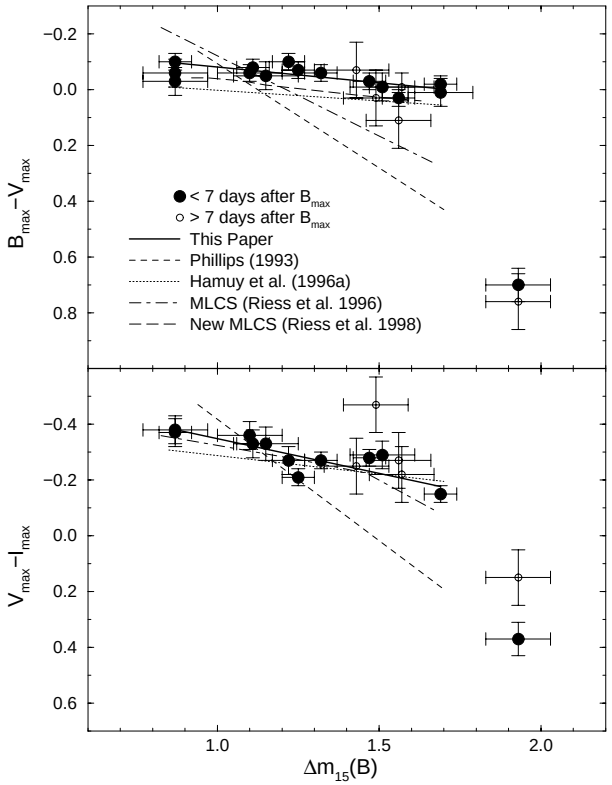

FIG. 5.—*Top*: $B_{max}-V_{max}$ "color" is plotted vs. the decline rate parameter $\Delta m_{15}(B)$ for 20 events with $E(B-V)_{Tail} < 0.06$. These SNe are likely to have little or no host galaxy reddening. *Bottom*: $V_{max}-I_{max}$ "color" is plotted vs. the decline rate parameter $\Delta m_{15}(B)$ for the same subsample of essentially unreddened SNe Ia.

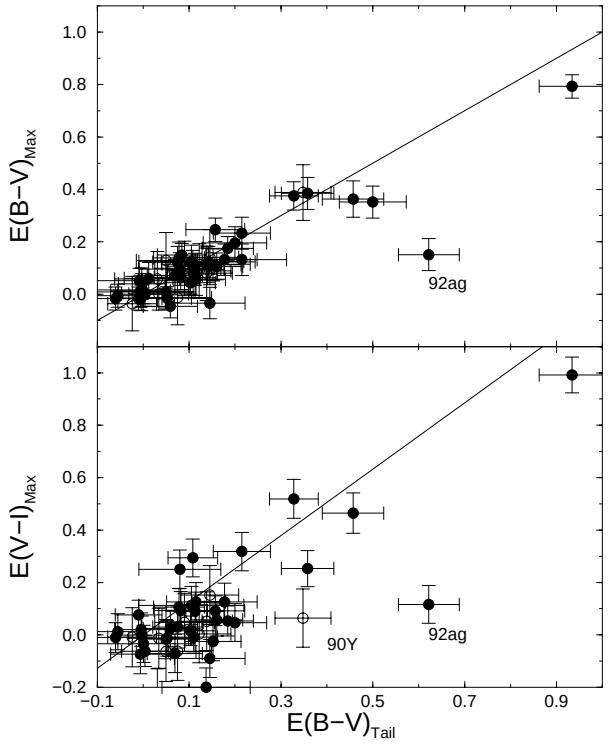

FIG. 6.—Comparison of color excesses calculated from the $B_{max}-V_{max}$ and $V_{max}-I_{max}$ colors vs. $E(B-V)_{tail}$. The solid line plotted in the lower panel assumes $E(V-I)_{max} = 1.25E(B-V)_{max}$, typical of dust in our own Galaxy. Open symbols correspond to SNe for which the first observation was not obtained until >7 days after the epoch of B_{max}.

iterative fashion, but the slopes of equations (7) and (8) are sufficiently shallow that this effect can be ignored for all but the most heavily reddened events. The observed color excesses are then converted to "true" color excesses via the following approximate relations:

$$E(B-V)_{true} = 0.981/[1/E(B-V)_{obs} - 0.050]\ , \quad (11)$$

$$E(V-I)_{true} = 0.989/[1/E(V-I)_{obs} - 0.004]\ . \quad (12)$$

Note that these color excesses, which we will refer to as $E(B-V)_{max}$ and $E(V-I)_{max}$, are valid only for SNe Ia with decline rates in the range $0.9 \le \Delta m_{15}(B) \le 1.6$ that also show "normal" spectra at maximum light—i.e., with strong Si II λ6355 absorption. In particular, this method should not be used to calculate reddenings for SN 1991T–like events that show very different spectra at maximum and therefore may have dissimilar intrinsic colors (e.g., see Phillips et al. 1992).

Values of $E(B-V)_{max}$ and $E(V-I)_{max}$ for the SNe in our sample are listed in columns (5)–(6) of Table 2 and are plotted versus $E(B-V)_{Tail}$ in Figure 6. Except for SN 1992ag, which we have already discussed, the agreement between $E(B-V)_{max}$ and $E(B-V)_{tail}$ is generally excellent. The relationship between $E(V-I)_{max}$ and $E(B-V)_{tail}$, while clearly significant, is not as impressive. Perhaps this is not surprising in view of the larger dispersion observed in the $E(V-I)_{max}$ versus $\Delta m_{15}(B)$ relation for relatively unreddened SNe Ia (see Fig. 5 and eq. [8]), which we suspect arises from two main causes: the generally poorer sampling of the I-band light curves for many of the Calán/Tololo SNe and the more complicated nature of the shapes of the I-band light curves, which makes predicting I_{max} from template fitting challenging. Nevertheless, we consider the $V_{max}-I_{max}$ color to be a useful alternative method of identifying significantly reddened SNe Ia.[5]

In column (7) of Table 2 we list the average color excess $E(B-V)_{Avg}$, which we take to be the weighted mean of $E(B-V)_{Tail}$, $E(B-V)_{max}$, and $0.8E(V-I)_{max}$. The multiplicative factor of 0.8 for $E(V-I)_{max}$ corresponds to an assumption of a standard Galactic interstellar reddening curve (Dean, Warren, & Cousins 1978; see also § 3). In addition, to handle negative reddening values, we have applied the "Bayesian filter" used by Riess et al. (1998), which assumes a one-sided Gaussian a priori distribution of A_B values with a maximum at zero and $\sigma = 0.3$ mag. For the subsample of 19 SNe Ia in E and S0 host galaxies with $0.9 \le \Delta m_{15}(B) \le 1.6$, we find

$$E(B-V)_{Avg} = 0.02 \pm 0.03,\ \sigma = 0.05,\ n = 21\ ,$$

which implies that the zero points of equations (1), (7), and (8) are reasonable and that the typical precision of a mea-

[5] Strictly speaking, color excesses estimated via equations (7) and (8) are not fully independent of the $E(B-V)_{tail}$ measurements for the same SNe, since a change in the zero point or slope of the Lira relation (eq. [1]) could change somewhat the exact sample of unreddened events used to derive equations (7) and (8). Also, an uncertainty in V_{max} will produce a correlated error in $E(B-V)_{max}$ and $E(V-I)_{max}$, since both use the same measurement.

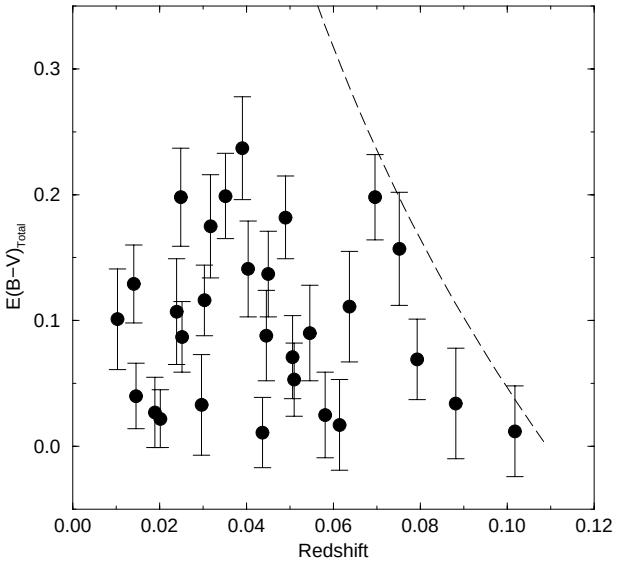

FIG. 7.—Total dust reddening (i.e., the sum of the Galactic and host galaxy contributions) plotted as a function of redshift for the 29 SNe Ia in the Calán/Tololo sample. The dashed line shows the upper limit to the allowed color excess for the limiting magnitude of this search, $B_{\rm Limit} = 19$.

surement of $E(B-V)_{\rm Avg}$ for any single SN Ia is ~ 0.05 mag. As expected, we find that the most reddened SNe were observed in spiral galaxies: 82% of the SNe with host galaxy reddenings greater than 0.05 mag occurred in spirals, whereas only 29% of the SNe with $E(B-V)_{\rm Avg} \leq 0.05$ mag had spiral galaxy hosts.

Figure 7 shows the total reddening, $E(B-V)_{\rm Avg}$, derived for the Calán/Tololo SNe Ia plotted as a function of host galaxy redshift. From the Hubble diagram fits given in § 3 and the definition of the observed magnitude of a supernova as $B_{\rm obs} = B_o + A_B$, it can easily be shown that the maximum allowed color excess for an SN as a function of redshift in a magnitude-limited search is

$$E(B-V) \simeq (B_{\rm limit} - 5 \log cz + 3.57)/4.1 \ . \qquad (13)$$

The dashed line in Figure 7 shows equation (13) plotted for the limiting magnitude of the Calán/Tololo search, $B_{\rm limit} \sim 19$ (Hamuy et al. 1993). This curve provides a good fit to the upper envelope of the observed reddenings, particularly at higher redshifts. The fact that SNe in a magnitude-limited search will have preferentially smaller dust reddenings as a function of redshift will naturally lead to a greater percentage of SNe being discovered in E/S0 galaxies at higher redshifts, exactly as is observed in the Calán/Tololo sample (Hamuy et al. 1996b). These results and predictions provide confidence in the validity of our techniques for measuring the reddenings of SNe Ia.

3. THE REDDENING-FREE DECLINE RATE VERSUS LUMINOSITY RELATION

Once the reddening of an SN Ia is known, correcting the observed maximum-light magnitudes for this extinction is straightforward. The general formula for a given filter is

$$m_0 = [m_{\rm obs} - A_m({\rm Gal})] - K_m - A_m({\rm host}) \ ,$$

where $m_{\rm obs}$ is the observed maximum-light magnitude, A_m(Gal) is the Galactic component of extinction, K_m is the K-correction (which, as noted in § 2.1, is a function of both redshift and reddening), and A_m(host) is the host galaxy component of extinction. From the data shown in Figure 2 and similar calculations for the V and I bands, the dependence of the extinction on color excess at maximum light can be approximated as

$$A_B = [4.16 - 0.06E(B-V)_{\rm true}]E(B-V)_{\rm true} \ , \qquad (14)$$

$$A_V = [3.14 - 0.02E(B-V)_{\rm true}]E(B-V)_{\rm true} \ , \qquad (15)$$

and

$$A_V = [1.82 + 0.01E(B-V)_{\rm true}]E(B-V)_{\rm true} \ . \qquad (16)$$

Equations (14)–(16) are valid for calculating either the Galactic or host galaxy components of the extinction.

The left half of Figure 8 shows the absolute magnitudes corrected only for Galactic reddening for the full sample of 29 Calán/Tololo and 12 CfA SNe, with $z \geq 0.01$ plotted as a function of the observed decline rate parameter $\Delta m_{15}(B)_{\rm obs}$. The distance to each SN was calculated from the redshift of the host galaxy (in the cosmic microwave background frame) and an assumed value of the Hubble constant of $H_0 = 65$ km s^{-1} Mpc^{-1}. Following Hamuy et al. (1996a), a peculiar velocity term of 600 km s^{-1} has been included in the error bars of the absolute magnitudes.

In the right half of Figure 8, this plot is repeated for the subsample of 18 of these 41 SNe for which we find insignificant host galaxy reddening [$E(B-V)_{\rm Avg} < 0.05$]. This diagram reveals more clearly than ever the true nature of the peak luminosity-decline rate relations for SNe Ia. Elimination of the events with significant host galaxy reddening not only decreases the scatter in the relations but also shows these to be nonlinear in the B and V bands and probably also in I. (Note that Riess et al. 1998 also found this dependence to be nonlinear and used a quadratic term in the revised MLCS.) In the right half of Figure 8, we plot for comparison as dashed lines the linear fits given by Hamuy et al. (1996a) for the 26 Calán/Tololo SNe with $B_{\rm max} - V_{\rm max} < 0.2$. These show best agreement in I, where reddening effects are smaller but are progressively worse approximations to the actual peak luminosity-decline rate relations in the V and B bands because of the combined effects of uncorrected host galaxy extinction and the curvature, which is apparent in the true relations.

For this "low host-galaxy reddening" subsample of the Calán/Tololo and CfA SNe with decline rates in the range $0.85 < \Delta m_{15}(B) < 1.70$, we calculated a least-squares fit to a quadratic peak luminosity-decline rate relation for the V-band data. This fit was then combined with equations (7) and (8) to give corresponding relations for the B and I bands. Table 3 lists the resulting parameters for these fits expressed in terms of the magnitude difference, $\Delta M_{\rm max}$, with respect to the maximum light magnitude of an SN with $\Delta m_{15}(B) = 1.1$. Note that the low values of χ^2_ν are probably

TABLE 3

FITS TO DECLINE RATE VERSUS LUMINOSITY RELATION[a]
$\Delta M_{\rm max} = a[\Delta m_{15}(B) - 1.1] + b[\Delta m_{15}(B) - 1.1]^2$

Bandpass	a[b]	b[b]	σ (mag)	χ^2_ν	Number
B.....	0.786(398)	0.633(742)	0.11	0.47	17
V	0.672(396)	0.633(742)	0.09	0.42	17
I	0.422(400)	0.633(742)	0.13	0.83	15

[a] $\Delta M_{\rm max} = M_{\rm max} - M_{\rm max}[\Delta m_{15}(B) = 1.1]$.
[b] Errors are listed in units of 0.001 mag.

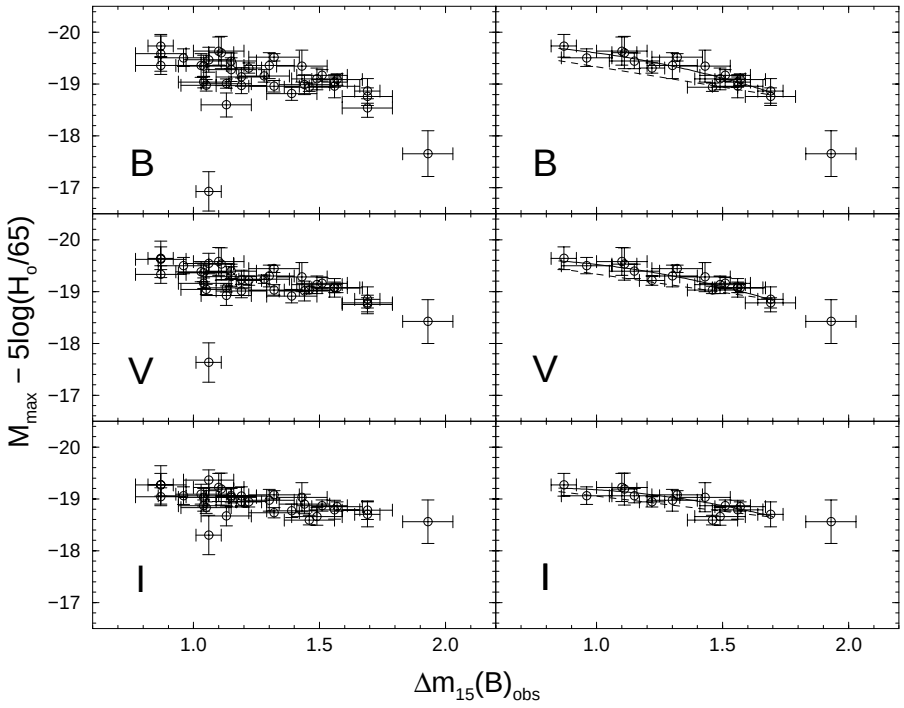

FIG. 8.—*Left*: Absolute *BVI* magnitudes corrected only for Galactic reddening plotted vs. the decline rate parameter $\Delta m_{15}(B)$ for the full sample of 41 Calán/Tololo and CfA SNe Ia with $z \geq 0.01$. *Right*: Same diagram after elimination of the 23 SNe in the sample for which we find significant host galaxy reddening. The dashed lines correspond to the linear fits given by Hamuy et al. (1996a).

due to an overestimate of the errors by Hamuy et al. (1996a), which we have adopted verbatim. The impressively low dispersions (0.09–0.13 mag) of these fits strongly support the validity of the methods described in this paper for estimating the host-galaxy dust reddening. For reference, Hamuy et al. (1996a), who employed a color cut of $B_{max} - V_{max} < 0.2$ and assumed linear relations for $\Delta m_{15}(B)$ versus M_{max}, obtained dispersions of 0.17, 0.14, and 0.13 mag for the fits in B, V, and I, respectively. The wavelength dependence of these values is due to a combination of uncorrected host galaxy extinction and the nonlinear shape of the $\Delta m_{15}(B)$ versus M_{max} relation in B and V; when these effects are taken into account, the dispersion is uniformly low in BVI.

From the average values of the host galaxy reddening given in Table 2 and the decline rate versus luminosity relations given in Table 3, we have reexamined the corrected Hubble diagrams in BVI for the 26 Calán/Tololo with $B_{max} - V_{max} < 0.2$, which Hamuy et al. (1996a, 1996b) referred to as their "low-extinction" sample. To provide an absolute calibration for these diagrams and, hence, an estimate of the Hubble constant, we use the same four SNe (1937C, 1972E, 1981B, and 1990N) with Cepheid distances employed by Hamuy et al. (1996b). Three different cases were considered, correcting for (1) Galactic reddening only, (2) Galactic reddening and the $\Delta m_{15}(B)$ versus M_{max} relation, and (3) Galactic reddening, host galaxy reddening, and the $\Delta m_{15}(B)$ versus M_{max} relation.

Averaging the results for BVI, we find the Hubble relations illustrated in Figure 9. (Note that the errors given in this figure for H_0 are internal only and do not include the external error due to uncertainties in the zero point of the Cepheid period-luminosity calibration, which we estimate

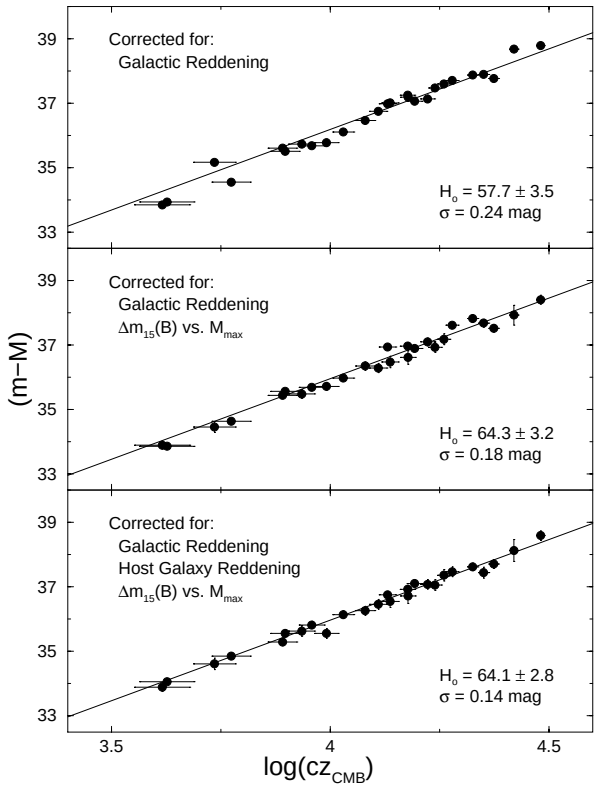

FIG. 9.—Hubble diagrams for the 26 SNe Ia in the Calán/Tololo "low-extinction" ($B_{max} - V_{max} < 0.2$) sample. The data are shown corrected for Galactic reddening only (*upper panel*), Galactic reddening and the $\Delta m_{15}(B)$ vs. M_{max} relation (*middle panel*), and Galactic reddening, host galaxy reddening, and the $\Delta m_{15}(B)$ vs. M_{max} relation (*lower panel*). The Hubble constants and dispersions derived for each case are indicated.

to be an additional 3–4 km s^{-1} Mpc^{-1}.) Not surprisingly, for the first two cases we find Hubble constants and dispersions that are similar to those given by Hamuy et al. (1996b) for comparable corrections. Note that case 1 is essentially the method employed by Sandage et al. (1996), who ignored the existence of the $\Delta m_{15}(B)$ versus $M_{\max}$ relation; the lower Hubble constant results from the fact that the average decline rate of the four calibrators with Cepheid distances [$\Delta m_{15}(B) = 0.97$] is significantly lower than the mean value for the 26 Calán/Tololo SNe [$\Delta m_{15}(B) = 1.24$], meaning that the calibrators are on average ~ 0.2 mag more luminous than the Calán/Tololo SNe. Correcting for the $\Delta m_{15}(B)$ versus $M_{\max}$ relation (case 2) eliminates this bias and significantly decreases the dispersion in the Hubble diagram. Applying the host-galaxy reddening corrections (case 3) decreases the dispersion still further, illustrating the merit of our approach to calculating these corrections, although we find essentially the same value of H_0 as when this correction is ignored (case 2). This is ascribed to the coincidence that the median reddening [$E(B-V)_{\rm host} = 0.05$ mag] of the 26 distant SNe happens to be virtually identical to the median reddening [$E(B-V)_{\rm host} = 0.06$ mag] for the four calibrating events.

From fits to the fully corrected [i.e., for Galactic + host-galaxy reddening and the $\Delta m_{15}(B)$ vs. $M_{\max}$ relations] magnitudes of our complete sample of 28 Calán/Tololo and 12 Cfa SNe with $z \geq 0.01$ and $\Delta m_{15}(B) < 1.70$, we find the following relations for the Hubble constant in BVI:

$$\log H_0(B) = 0.2\{M^B_{\max} - 0.786(\pm 0.398) \times [\Delta m_{15}(B) - 1.1] - 0.633(\pm 0.742) \times [\Delta m_{15}(B) - 1.1]^2 + 28.671(\pm 0.043)\} , \quad (17)$$

$$\log H_0(V) = 0.2\{M^V_{\max} - 0.672(\pm 0.396) \times [\Delta m_{15}(B) - 1.1] - 0.633(\pm 0.742) \times [\Delta m_{15}(B) - 1.1]^2 + 28.615(\pm 0.037)\} , \quad (18)$$

$$\log H_0(I) = 0.2\{M^I_{\max} - 0.422(\pm 0.400) \times [\Delta m_{15}(B) - 1.1] - 0.633(\pm 0.742) \times [\Delta m_{15}(B) - 1.1]^2 + 28.236(\pm 0.035)\} . \quad (19)$$

Combining equations (17)–(19) with the corrected absolute magnitudes of the six well-observed SNe Ia (1937C, 1972E, 1981B, 1989B, 1990N, 1998bu—see Saha et al. 1999 and Suntzeff et al. 1999 for details and references) with *Hubble Space Telescope* Cepheid distances gives a value of the Hubble constant of 63.3 ± 2.2(internal) $\pm$ 3.5(external) km s^{-1} Mpc^{-1}. Until more Cepheid distances become available for nearby, well-observed events, this value represents our best estimate for the Hubble constant.

Finally, we briefly address the question of whether the extinction law of the host galaxy dust affecting SNe Ia is consistent with that typically observed for dust in the disk of our own Galaxy. Using their original formulation of MLCS, Riess, Press, & Kirshner (1996b) concluded that this *was* the case, but since this same version of MLCS incorrectly predicted a strong relation between light-curve shape and the $B-V$ color at maximum light, it is worth reexamining the issue. We do this by plotting the absolute magnitudes of the SNe in our sample versus the $B_{\max}-V_{\max}$ color. However, because both of these quantities are a function of the decline rate, we must first correct them to a "standard" decline rate [we choose $\Delta m_{15}(B) = 1.1$] using the coefficients of the decline-rate–dependent portions of the relations given in Table 3 and equation (7). Specifically, we calculate

$$M(B)_{1.1} = M(B)_{\max} - 0.786[\Delta m_{15}(B) - 1.1] + 0.633[\Delta m_{15}(B) - 1.1]^2 , \quad (20)$$

$$M(V)_{1.1} = M(V)_{\max} - 0.672[\Delta m_{15}(B) - 1.1] + 0.633[\Delta m_{15}(B) - 1.1]^2 , \quad (21)$$

$$M(I)_{1.1} = M(I)_{\max} - 0.422[\Delta m_{15}(B) - 1.1] + 0.633[\Delta m_{15}(B) - 1.1]^2 , \quad (22)$$

and

$$(B_{\max}-V_{\max})_{1.1} = (B_{\max}-V_{\max}) - 0.114[\Delta m_{15}(B) - 1.1] . \quad (23)$$

These quantities are plotted in Figure 10 for the subsample of Calán/Tololo and CfA SNe Ia with $z \geq 0.01$ for which distances were calculated assuming $H_0 = 63.3$ and also for the SNe Ia with Cepheid-based host galaxy distances. In both cases, the samples were restricted to those events with light-curve coverage beginning ≤ 5 days after $B_{\max}$ and for which we have derived nonzero values of

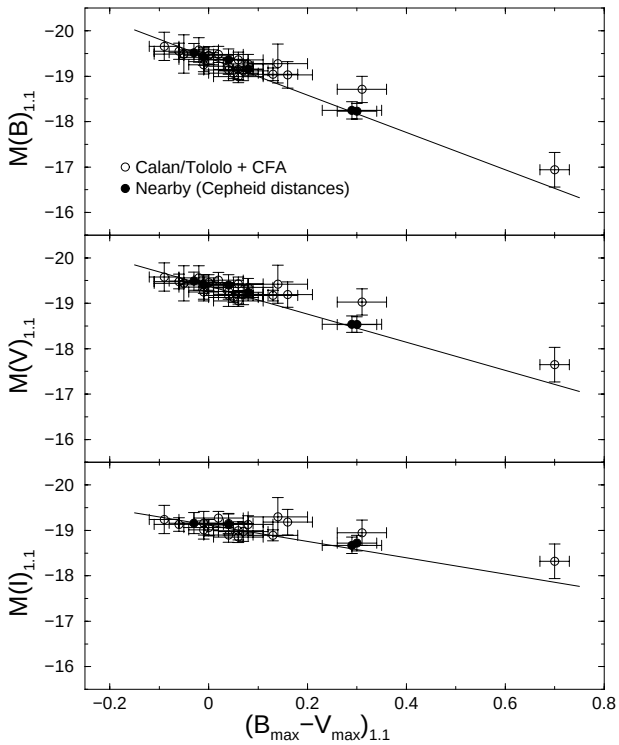

FIG. 10.—SN Ia absolute magnitudes plotted vs. $B_{\max}-V_{\max}$ for two samples consisting of the Calán/Tololo + CfA SNe Ia with $z \geq 0.01$ and nearby SNe Ia for which distances have been determined via Cepheids. Distances to the former set of objects were calculated assuming $H_0 = 63.3$. The decline rate dependence of both the absolute magnitudes and the $B_{\max}-V_{\max}$ color have been removed via equations (20)–(23). For both samples, only those SNe with light-curve coverage beginning ≤ 5 days after the epoch of $B_{\max}$ were considered. The canonical Galactic reddening vectors are illustrated as solid lines.

$E(B-V)_{\rm Avg}$. Plotted in Figure 10 for reference are the canonical Galactic reddening vectors with slopes of 4.1 in B, 3.1 in V, and 1.8 in I. A linear least-squares fit to the data gives slopes of 3.5 ± 0.4, 2.6 ± 0.4, and 1.2 ± 0.4, which agree to within ~ 1–$1.5\ \sigma$ with the Galactic values and are consistent with typical values of R observed in nearby galaxies (e.g., Hodge & Kennicutt 1982; Bouchet et al. 1985; Iye & Richter 1985; Brosch & Loinger 1988). Hence, we conclude that the host galaxy dust is similar in its properties, on average, to the dust in our own Galaxy.

4. CONCLUSIONS

In this paper we have presented methods for estimating the host galaxy dust extinction of SNe Ia at late times ($30 \leq t_V \leq 90$), when the $B-V$ evolution is remarkably similar for all events, and at maximum light where the colors $B_{\rm max}-V_{\rm max}$ and $V_{\rm max}-I_{\rm max}$ for normal-spectra SNe Ia display only a mild dependence on light-curve shape. From this, we are able to deduce the reddening-free relations in BVI for the dependence of absolute magnitude on the decline rate parameter $\Delta m_{15}(B)$. Fits to these data yield remarkably low dispersions (0.09–0.13 mag) in all three colors and lead to a revised value of the Hubble constant of $H_0 = 63.3 \pm 2.2$(internal) $\pm$ 3.5(external) km s^{-1} Mpc^{-1}.

We thank Adam Riess for his valuable comments on this paper and for providing the new MLCS fit in Figure 5. J. M. acknowledges support from "Cátedra Presidencial de Ciencias 1995" and FONDECYT grant 1980172.

REFERENCES

Ardeberg, A. L., & de Grood, M. J. 1973, A&A, 28, 295
Barbon, R., Ciatti, F., & Rosino, L. 1982, A&A, 116, 35
Blanco, V. M. 1956, ApJ, 123, 64
Bouchet, P., Lequeux, J., Maurice, E., Prevot, L., & Prevot-Burnichon, M. 1986, A&A, 149, 330
Brosch, N., & Loinger 1988, A&A, 249, 327
Burstein, D., & Heiles, C. 1982, AJ, 87, 1165
Buta, R. J., & Turner, A. 1983, PASP, 95, 72
Cardelli, J., Clayton, G., and Mathis, J. 1989, ApJ, 345, 245
Cousins, A. W. J. 1972, IBVS, 700
Dean, J. F., Warren, P. R., & Cousins, A. W. J. 1978, MNRAS, 183, 569
Filippenko, A. V., et al. 1992, AJ, 104, 1543
Goudfrooij, P., & de Jong, T. 1995, A&A, 298, 784
Hamuy, M., et al. 1996c, AJ, 112, 2408
Hamuy, M., Phillips, M. M., Maza, J., Suntzeff, N. B., Schommer, R. A., & Avilés, R. 1995, AJ, 109, 1
Hamuy, M., Phillips, M. M., Maza, J., Wischnjewsky, M., Uomoto, A., Landolt, A. U., & Khatwani, R. 1991, AJ, 102, 208
Hamuy, M., Phillips, M. M., Schommer, R. A., Suntzeff, N. B., Maza, J., & Avilés, R. 1996a, AJ, 112, 2391
Hamuy, M., Phillips, M. M., Suntzeff, N. B., Schommer, R. A., Maza, J., & Avilés, R. 1996b, AJ, 112, 2398
Hamuy, M., Phillips, M. M., Wells, L., & Maza, J. 1993, PASP, 105, 787
Hodge, P., & Kennicutt, R. 1982, AJ, 87, 264
Iye, M., & Richter, O. 1985, A&A, 144, 471
Kim, A. 1997, in Supernova Explosions: Their Causes and Consequences, ed. A. Burrows, K. Nomoto, & F. Thielemann (http://www.itp.ucsb.edu./online/supernova/snovaetrans.html)
Lee, T. A., Wamsteker, W., Wisniewski, W. Z., & Wdowiak, T. J. 1972, ApJ, 177, L59
Leibundgut, B. 1988, Ph.D. thesis, Univ. Basel
Leibundgut, B., et al. 1993, AJ, 105, 301
Lira, P. 1995, Masters thesis, Univ. Chile
Lira, P., et al. 1998, AJ, 115, 234
Nugent, P., et al. 1998, in preparation
Nugent, P., Phillips, M., Baron, E., Branch, D., & Hauschildt, P. 1995, ApJ, 455, L147
Perlmutter, S., et al. 1995, ApJ, 440, L41
Phillips, M. M. 1993, ApJ, 413, L105
Phillips, M. M., et al. 1987, PASP, 99, 592
Phillips, M. M., Wells, L., Suntzeff, N., Hamuy, M., Leibundgut, B., Kirshner, R. P., & Foltz, C. 1992, AJ, 103, 1632
Pierce, M. J., & Jacoby, G. H. 1995, AJ, 110, 2885
Riess, A. G., et al. 1998, AJ, 116, 1009
———. 1999, AJ, in press
Riess, A. G., Press, W. H., & Kirshner, R. P. 1995, ApJ, 438, L17
———. 1996a, ApJ, 473, 88
———. 1996b, ApJ, 473, 588
Saha, A., Sandage, A., Tammann, G. A., Labhardt, L., Macchetto, F. D., & Panagia, N. 1999, ApJ, in press
Sandage, A., Saha, A., Tammann, G. A., Labhardt, L., Panagia, N., & Macchetto, F. D. 1996, ApJ, 460, L15
Schlegel, D., Finkbeiner, D., & Davis, M. 1998, ApJ, 500, 525
Schmidt-Kaler, T. 1982, in Landolt-Börnstein New Series, Group 6, Vol. 2b, Stars and Star Clusters, ed. K. Schaifers & H.-H. Voigt (Berlin: Springer), 453
Suntzeff, N. B., et al. 1999, AJ, 117, 1175
Tsvetkov, D. Y. 1982, Soviet Astron. Lett., 8, 115
Wells, L. A., et al. 1994, AJ, 108, 2233
Wise, M. W., & Silva, D. R. 1996, ApJ, 461, 155